Journal of Applied Fluid Mechanics, Vol. 11, No. 3, pp. 621-635, 2018.
Available online at www.jafmonline.net, ISSN 1735-3572, EISSN 1735-3645.
DOI: 10.29252/jafm.11.03.27836

A Dramatic Enhancement of Heat Transfer in Dream Pipe with Viscoelastic Fluids

P. Puvaneswari and K. Shailendhra†

Department of Mathematics, Amrita Vishwa Vidya Peetham Coimbatore, India.

†*Corresponding Author Email: k shailendhra@cb.amrita.edu*

(Received April 3, 2017; accepted December 5, 2017)

ABSTRACT

A mathematical investigation on the combined effect of oscillation and conjugation on the enhancement of heat transfer in a heat pipe called Dream Pipe is carried out, when viscoelastic fluids (CPyCl/NaSal) are employed as the heat carriers. Closed-form solutions for the momentum and heat equations are presented. The physical and thermal properties of the polymer solution used are obtained by experiments. The effects of thermal conductivity and thickness of the wall, fluid thickness, Womersley number (α), Deborah number and Prandtl number on the enhancement of heat transfer are examined. Results obtained in the present analysis are in excellent agreement with those of the existing literature. The effective thermal diffusivity (κ_e) is maximized at optimum α where the fluid flow exhibits a resonant behavior. Several maxima occur in κ_e for several resonant frequencies and the dramatic increase in κ_e due to oscillation for the viscoelastic fluid is 5.63 x 10^9 times higher than that obtained by the molecular motion. This increase is much higher than that (1.84 x 10^4 times) obtained for the Newtonian fluid. κ_e is increased with increasing wall thermal conductivity and thickness in the viscous regime whereas in the elastic regime the effect of conjugation is saturated. In the viscous regime, a maximum increase of 50.63% in κ_e is obtained by optimizing the wall thickness. Also κ_e increases with increasing molar ratio of concentrations of counterion to surfactant. A maximum heat flux of 4.54 x 10^{10} W/m^2 is achieved using a viscoelastic fluid with thermally conducting wall and this highest heat flux is 207 times higher than that (2.19 x 10^8 W/m2) obtained with the Newtonian fluid (liquid metal). Hence, viscoelastic fluids are preferable to liquid metals as working fluids in the Dream Pipe. The new insights gained by the present investigation are useful while designing viscoelastic Dream Pipes and micro channel heat exchangers.

Keywords: Enhancement of Heat Transfer, Dream Pipe, Conjugate Heat Transfer, Laminar Oscillatory Flow, Viscoelastic Fluids, Molar Ratio.

NOMENCLATURE

a	pipe radius
A	cross-sectional area of the tube
A_o	amplitude of pressure gradient
b	half the wall thickness
c_f	specific heat capacity of the fluid
c_s	specific heat capacity of the plate
De	Deborah number
k_f	thermal conductivity of the fluid
k_s	thermal conductivity of the plate
k	thermal conductivity ratio
K_f	thermal diffusivity of the fluid
K_s	thermal diffusivity of the plate
p	pressure
P_r	Prandtl number
$\vec{q}$	velocity vector of the fluid
Q	Heat flux due to convection
Q_m	Heat flux due to conduction
r	radial coordinate
t	dimensional time
t_m	fluid relaxation time
T	temperature
u	dimensional velocity component along x axis
U	non-dimensional velocity component along x axis
x	x axial coordinate
α	Womersley number
ε	non-dimensional wall thickness
γ	constant axial temperature gradient
κ_e	dimensional effective (enhanced) thermal diffusivity of the fluid
κ_e^*	non-dimensional effective (enhanced) thermal diffusivity of the fluid
κ_f	thermal diffusivity of the fluid
κ_s	thermal diffusivity of the plate
λ	non-dimensional magnitude of imposed sinusoidal pressure gradient
μ	dynamic viscosity

v	kinematic viscosity of the fluid	τ	non dimensional time
ρ	density of the fluid	ω	oscillation frequency
σ	thermal diffusivity ratio		

1. INTRODUCTION

Enhancement of heat transfer in fluids plays a significant role in the design of many traditional heat transfer devices like heat exchangers and cooling modules. There are different enhancement techniques among which the oscillation technique is the best one and it can improve a given transport process. For instance, the axial dispersion of contaminants within laminar oscillatory flows through capillary tubes is considerably larger than that obtained by pure molecular diffusion in the absence of flow (Chatwin 1975; Watson 1983). In view of mathematical similarity between the diffusion and heat conduction equations, this technique was adopted by Kurzweg (Kurzweg and De Zhao 1984; Kurzweg 1985a; Kurzweg 1985b) in a sinusoidal oscillatory flow through circular tubes connecting two fluid reservoirs maintained at different temperatures for enhancement of heat transfer. The super-position of sinusoidal oscillations on the fluid produces a considerable increase in axial heat transport between the reservoirs without a net mass transfer. The existence of such an enhanced heat transfer was confirmed experimentally by Kurzweg and Zhao (Kurzweg and De Zhao 1984) in the Newtonian fluid through capillary tubes connecting two cylindrical containers with different temperatures. It was showed that large quantities of heat can be transported axially provided the fluid is oscillated at high frequency and with large tidal displacements. A heat flux of 0.6 x 10^{10} W/m^2 was obtained with oscillating liquid lithium within a metallic capillary bundle, each with a radius of 5 x 10^{-2} cm at a frequency of 50 Hz with a tidal displacement of 100 cm if 4^{o}C/cm temperature gradient is maintained along the axis (Patent No: US 4,590,993, May, 1986). Later, Kurzweg (Kurzweg 1985b) investigated this enhancement of heat transfer in the flow of a Newtonian fluid in an array of parallel plate channels with conducting side walls. Large heat transfer rates in excess of 10^{10} W/m^2 were achieved by this process. Moreover, Kurzweg designed a novel heat transfer device (Patent No: US 4,590,993, May, 1986) called dream pipe for the enhancement of heat transfer which is more excellent than ordinary heat pipes. In fact, an axial heat flux of 1.3 x 10^{10} W/m^2 could be achieved by using liquid sodium as a heat transfer fluid at an oscillation amplitude of 100 cm at a frequency of 30 Hz in metal tubes of 0.4 mm diameter each. The admirable features of this dream pipe are well explained in (Shailendhra and AnjaliDevi 2011). The basic idea of this device is to transfer heat at higher rates, without concomitant net mass transfer, by sinusoidal oscillation of liquid metals, under laminar conditions, when a constant axial temperature gradient is maintained. This thermal pumping technique introduced by Kurzweg finds applications in cooling of radioactive liquids, hazardous chemical solutions, thermal valves and also in the field of cryogenics (Kurzweg 1986).

In this context, it is very much interesting and extremely advantageous to consider the possibility of using non Newtonian viscoelastic fluids rather than Newtonian fluids for heat transfer applications. Viscoelastic fluids are used in applications such as district cooling, oil and gas production and consumer products (Wanwipa Siriwatwechakul and Sullivan 2004). In large scale heating and cooling installations, viscoelastic fluids are used to decrease the pumping power requirements and hence to increase the efficiency of the system by providing drag reduction. It is advantageous to use the viscoelastic surfactant solutions over polymeric additives as the self-heating surfactant micelles do not irreversibly shear-degrade whereas polymers may do that (Wanwipa Siriwatwechakul and Sullivan 2004). In fact, the laminar flow of a non Newtonian viscoelastic fluid between two parallel plates was investigated by Kurtcebe and Erim (Kurtcebe and Erim 2005). It was found that the wall friction decreases in case a viscoelastic coolant is used and that the Nusselt number decreases in the case of a Newtonian fluid. However, the problem on the heat transfer in concentric annular flows of viscoelastic fluids was modeled by Pinho and Celho (Pinho and Coelho 2006). They showed that the heat transfer rate is increased by the fluid elasticity and the internal heat generation due to viscous dissipation and that the heat transfer rate is increased when the viscous dissipation is strong. The enhancement of heat transfer in a laminar flow of non-Newtonian fluids flowing through rectangular ducts was examined by Monica F. Naccache and Paulo R. Souza Mendes (Naccache and Mendes 1996). It was found that heat transfer in a non-Newtonian viscoelastic fluid is strongly enhanced by secondary flows which occur due to the elastic behavior of the fluid and that the values of the Nusselt number are three times larger than those for the Newtonian flu-ids. The heat transfer performance of viscoelastic fluid (Polyacrylamide water solution) flowing through a serpentine channel with square cross-section under low Reynolds number conditions was analysed by Kazuya Tatsumi *et al* (Tatsumi, Nakajima, Nagasaka, and Nakabe 2012). Considerable enhancement of heat transfer performance was obtained by the flow fluctuation and longitudinal vortices and the generation of these vortices was attributed to the normal stress produced by the viscoelasticity of the fluid and the curvature of the channel. An investigation on convective heat transfer with viscoelastic fluids in a rectangular duct was executed by N. Peres *et al* (Peres, Afonso, Alves, and Pinho 2009) to analyze the effect of secondary flow on the heat transfer enhancement. The generators of this heat transfer enhancement are the fluid rheology, especially the shear-thinning nature of the viscoelastic fluid and the existence of

the secondary flow produced by the non-zero second normal stress differences. The enhancement of heat transfer in a rectangular micro channel with constant wall heat flux was studied by Zhou Guo Fa and Peng Ting (Zhou and Peng 2012), using numerical simulation method. The simulation results showed that the maximum heat transfer enhancement of viscoelastic fluid is up to 800 %, compared with pure vis-cous fluid. Lambert *et al* (Lambert, Cuevas, and Del Rio 2006) examined the heat transfer process that takes place in a straight tube connecting a solar collector with the heat reservoir. They explored the behavior using both Newtonian and viscoelastic fluids. Several maxima of the effective thermal diffusivity for different resonant frequencies were observed for the viscoelastic fluid whereas there is a single maximum value of effective thermal diffusivity for a specific oscillation frequency in the case of Newtonian fluid. Further, the enhancement of heat transfer in a laminar oscillatory flow of Newtonian and viscoelastic fluids in a long tube of circular cross section with nonconducting walls has been analysed by Lambert *et al* (Lambert, Cuevas, Del Rio, and de Haro 2009). They have reported that the absolute maximum of the enhanced thermal diffusivity for the viscoelastic fluid and consequently the axial heat transfer in the tube is much higher than those for the Newtonian fluid. These heat transfer studies with non-Newtonian viscoelastic fluids motivated us to use the non Newtonian viscoelastic fluids in the present analysis.

On the other hand several authors have considered the enhancement of heat transfer in the laminar oscillatory flows with conjugate effect as the wall properties like its thickness and thermal conductivity also influence the heat flux transported by the fluid. Kurzweg and Zhao (Kurzweg and De Zhao 1984) considered three interesting cases of zero, in-finite wall thermal conductivity and the case where the fluid and the wall have the same thermal conductivities and thermal diffusivities. They reported that the amount of heat transported is larger when the thermal conductivity of the wall is higher. Even though Kurzweg modeled the problem (Kurzweg 1985b) as a conjugate heat transfer problem, the effect of conjugation was not addressed. The same problem of Kurzweg was extended by Kaviany (Kaviany 1986) by considering the effects of viscous dissipation, the presence of harmonics other than the fundamental harmonics, channel spacing and wall thickness. With mercury as the working fluid and aluminum and glass as the wall material it was showed that the effective thermal diffusivity increases with increasing wall thickness when the frequency ranges from 1 to 10^3 (rad/s). Longitudinal heat transfer enhanced by fluid oscillation in a circular tube with conductive wall was investigated by Inaba *et al*., (Inaba, Morita, and Saitoh 2004). With water as the working fluid, acrylic, copper and glass as the wall materials they observed that the heat transfer through the fluid is more enhanced with increasing conductivities of the wall up to a certain wall thickness. Recently, Puvaneswari and Shailendhra (Puvaneswari and Shailendhra 2016) have studied this conjugation effect on the enhancement of heat transfer in a laminar liquid metal flow past a thermally conducting and sinusoidally oscillating infinite flat plate with finite thickness and concluded that a maximum increase of 46.14% in heat flux can be achieved by optimizing the wall thickness and that a maximum total heat flux of 1.87 x 10^8 W/m^2 can be obtained using Na with AISI 316 wall. The previous problem has been ex-tended to the magnetic case by Puvaneswari and Shailendhra (Puvaneswari and Shailendhra 2017a) by applying a uniform transverse magnetic field perpendicular to the direction of oscillation of the plate. Due to oscillation the heat flux can be enhanced by O (10^3) and a maximum increase of 52.03 % in heat flux has been obtained by optimizing the wall thickness in the presence of magnetic field. In all the above conjugate heat transfer problems, the working fluid is a Newtonian fluid. To our knowledge heat transfer enhancement in non -Newtonian viscoelastic oscillatory flow in circular tubes with thermally conducting walls has not been dealt with. Hence, in the present analysis, we have extended the problem (Lambert, Cuevas, Del Rio, and de Haro 2009) to the conjugate case and analysed the combined effects of conjugation and oscillation on the enhancement of heat transfer. Our main aim of the present study is not only to analyse the effect of conjugation on the enhancement of heat transfer but also to determine whether the utility of viscoelastic fluids in the enhancement of heat transfer process leads to the existence of multiple resonant frequencies for which the effective thermal diffusivity display maximum values which are several orders of magnitude higher than those for Newtonian fluid in the conjugate case also. In such a case viscoelastic fluids would be the suitable working fluids in the conjugate heat transfer problems pertaining to the enhancement of heat transfer.

2. MATHEMATICAL FORMULATION AND SOLUTION

Consider the laminar axisymmetric flow of a viscoelastic fluid, induced by a sinusoidal pressure gradient in a tube of radius a and length L whose ends are connected to two reservoirs of constant but different temperatures ie., T (x = 0) = T_1 and T (x = L) = T_2. The axis of the fluid motion is x, which is the direction of the applied pressure gradient. The walls of the tube are assumed to be thermally conducting with finite thickness. The fluid thickness and the wall thickness are assumed to be 2a and 2b respectively. The temperature gradient is maintained as a constant (=γ) within the fluid and the walls. The schematic representation of the problem is given in Fig. 1.

The continuity equation is

$$\nabla \cdot \vec{q} = 0 \tag{1}$$

where $\vec{q}$ is the velocity of the fluid represented as $\vec{q}$ = [u,0,0] which gives

$$\frac{\partial u}{\partial x} = 0 \tag{2}$$

and hence u = u(r,t). The momentum equation is

$$\rho_f \frac{\partial \vec{q}}{\partial t} + \rho_f \left(\vec{q} \cdot \nabla\right)\vec{q} = -\nabla p - \nabla \cdot \vec{\tau}, \tag{3}$$

where ρ_f is the density of the fluid, p, the pressure and $\vec{\tau}$ is the viscous stress tensor.

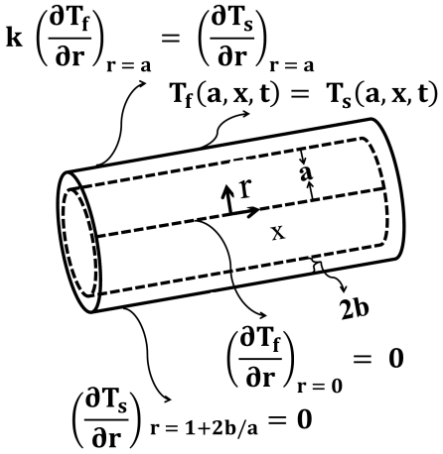

Fig. 1. Schematic representation of the problem.

We assume that $\vec{\tau}$ satisfies the linear form of the Maxwell model (Lambert, Cuevas, and Del Rio 2006), namely

$$t_m \frac{\partial \vec{\tau}}{\partial t} = -\mu \nabla \vec{q} - \vec{\tau} \tag{4}$$

where t_m represents the fluid relaxation time and μ is the kinematic coefficient of viscosity of the fluid.

Using (3) in (4), (4) becomes

$$t_m \frac{\partial^2 u}{\partial t^2} + \frac{\partial u}{\partial t} = \frac{-1}{\rho}\left[t_m \frac{\partial}{\partial t}\left(\frac{\partial p}{\partial x}\right) + \frac{\partial p}{\partial x}\right] + \frac{\mu}{\rho_f}\left\{\frac{1}{r}\frac{\partial}{\partial r}\left(r\frac{\partial u}{\partial r}\right)\right\} \tag{5}$$

The boundary conditions for the velocity are $\frac{\partial u}{\partial r}(0,t) = 0$ and $u(a,t) = 0$

These conditions correspond to the axial symmetry of the velocity profile and the nonslip condition at the wall.

We assume that the zero mean oscillatory flow is driven by a harmonic pressure gradient which can be expressed as the real part of $\frac{\partial p}{\partial x} = A_0 e^{-i\omega t}$ where A_0 is the constant amplitude of the pressure gradient.

Using the dimensionless parameters $R = \frac{r}{a}, U = \frac{u}{U_0}, \tau = \omega t$ and $\lambda = \frac{A_0 a^2}{\rho \nu U_0}$ into Eq (5), (5) becomes

$$\omega t_m \frac{\partial^2 U}{\partial \tau^2} + \frac{\partial U}{\partial \tau} = \frac{-\lambda}{\alpha^2}\left[1 - i\omega t_m\right]e^{-i\tau} + \frac{1}{\alpha^2}\left\{\frac{\partial^2 U}{\partial R^2} + \frac{1}{R}\frac{\partial U}{\partial R}\right\} \tag{6}$$

where $\alpha = \sqrt{a^2\omega/\nu}$ is the Womersley number. The boundary conditions in non-dimensional form are given by

$$\frac{\partial U}{\partial R} = 0 \ \textit{when R=0} \tag{7}$$

$$\textit{U=0 when R=1} \tag{8}$$

Assuming $U(R,\tau) = \mathrm{Re}\left\{V(R)e^{-i\tau}\right\}$, from (6) we obtain

$$\frac{\partial^2 V}{\partial R^2} + \frac{1}{R}\frac{\partial V}{\partial R} + \alpha^2\left(\omega t_m + i\right)V = \lambda\left(1 - i\omega t_m\right)$$

The solution of the above equation that satisfies the boundary conditions (7) and (8) is given by

$$V(R) = \frac{-i\lambda}{\alpha^2}\left[1 - \frac{J_0(\beta_v R)}{J_0(\beta_v)}\right]$$

and therefore

$$U(R,\tau) = \mathrm{Re}\left\{\frac{-i\lambda}{\alpha^2}\left[1 - \frac{J_0(\beta_v R)}{J_0(\beta_v)}\right]e^{-i\tau}\right\} \tag{9}$$

where $\beta_v = \alpha\sqrt{\omega t_m + i}$ and $\beta_v^2 = \alpha^2\left(\alpha^2 D_e + i\right)$

Here, $D_e = \frac{\mu t_m}{a^2\rho_f}$ is the Deborah number that measures the ratio of the relaxation time t_m to the viscous diffusion time $\frac{a^2\rho_f}{\mu}$ and J_0 is the cylindrical zeroth order Bessel function of the first kind. The tidal displacement (Δx) representing the cross-stream averaged maximum axial distance which the fluid elements travel during one half period of oscillation is given by

$$\Delta x = \left|\frac{1}{A}\int_{\frac{-\pi}{2\omega}}^{\frac{\pi}{2\omega}}\int_0^{2\pi}\int_0^a u(r,t)\,r\,dr\,d\theta\,dt\right| \tag{10}$$

where $A = \pi a^2$ is the cross sectional area of the tube.

Introducing (9) into (10) and carrying out the integration, we get

$$\Delta x = \frac{2U_0\lambda}{\omega a^2}\left|\mathrm{Re}\left(1 - \frac{2J_1(\beta_v)}{\beta_v J_0(\beta_v)}\right)\right|$$

where J_1 is the Bessel function of the first kind and first order.

The fluid temperature is described by the heat equations in the fluid and wall which are given by

$$\frac{\partial T_f}{\partial t}+u(r,t)\frac{\partial T_f}{\partial x}=\kappa_f\left(\frac{\partial^2 T_f}{\partial r^2}+\frac{1}{r}\frac{\partial T_f}{\partial r}+\frac{\partial^2 T_f}{\partial x^2}\right), 0 < r < a$$

$$\frac{\partial T_s}{\partial t}=\kappa_s\left(\frac{\partial^2 T_s}{\partial r^2}+\frac{1}{r}\frac{\partial T_s}{\partial r}+\frac{\partial^2 T_s}{\partial x^2}\right),$$

$$a < r < a+2b$$

Assuming $\frac{\partial T_f}{\partial x}=\gamma\left(cons\tan t\right)=\frac{\partial T_s}{\partial x}$ the above equations are expressed in non-dimensional form as

$$\frac{\partial T_f}{\partial \tau}(R,x,\tau)+\frac{U_0 U}{\omega}\gamma=\frac{1}{\alpha^2\,\mathrm{Pr}}\left(\frac{\partial^2 T_f}{\partial R^2}+\frac{1}{R}\frac{\partial T_f}{\partial R}\right),$$

$$0 < R < 1 \qquad (11)$$

$$\frac{\partial T_s}{\partial \tau}(R,x,\tau)=\frac{1}{\alpha^2\sigma\,\mathrm{Pr}}\left(\frac{\partial^2 T_s}{\partial R^2}+\frac{1}{R}\frac{\partial T_s}{\partial R}\right),$$

$$1 < R < 1+2\varepsilon \qquad (12)$$

The boundary conditions in the non dimensional form are given by

$$T_f(0,x,\tau)=finite \qquad (13)$$

$$T_f(1,x,\tau)=T_s(1,x,\tau) \qquad (14)$$

$$k\left(\frac{\partial T_f}{\partial R}\right)_{R=1}=\left(\frac{\partial T_s}{\partial R}\right)_{R=1}, k=\frac{k_f}{k_s}, \qquad (15)$$

$$\left(\frac{\partial T_s}{\partial R}\right)_{R=1+2\varepsilon}=0, \varepsilon=\frac{b}{a} \qquad (16)$$

These conditions correspond to the finite temperature at the axis R = 0 of the pipe, continuity of temperature at the fluid solid interface R = 1, continuity of heat flux at the fluid solid interface R = 1 and the insulated boundary condition at the outer boundary

R = 1 + 2ε of the wall respectively. Assuming that $T_f(R,x,\tau)=\gamma\,\mathrm{Re}\left(x+\phi(R)e^{-i\tau}\right)$ and substituting this and (9) into (11), (11) yields

$$\frac{d^2\phi(R)}{dR^2}+\frac{1}{R}\frac{d\phi(R)}{dR}+i\alpha^2\,\mathrm{Pr}\,\phi(R)=\frac{-i\lambda U_0\,\mathrm{Pr}}{\omega}\left(1-\frac{J_0(\beta_v R)}{J_0(\beta_v)}\right) \qquad (17)$$

which is a non homogeneous zeroth order Bessel equation.

The general solution of (17) is given by

$$\phi(R)=A_1 J_0\left(\beta_{T_f}R\right)+A_2 Y_0\left(\beta_{T_f}R\right)+\phi_p(R) \qquad (18)$$

where $\beta_{T_f}^2=i\alpha^2\,\mathrm{Pr}$, Y_0 is the Bessel function of the second kind and zeroth order and $\varphi_P(R)$ is obtained by the method of undetermined coefficients which is given by

$$\phi_p(R)=-\frac{i\lambda U_0\,\mathrm{Pr}\,J_0(\beta_v R)}{\omega\left(\beta_v^2-\beta_{T_f}^2\right)J_0(\beta_v)}-\frac{i\lambda U_0\,\mathrm{Pr}}{\omega\beta_{T_f}^2}$$

From (13) we have $\varphi(0) = finite$. When $R \to 0$, $Y_0\left(\beta_{T_f}R\right)\to-\infty$ and hence $\varphi(R) \to -\infty$ which is not possible. Therefore, we set $A_2 = 0$.

Hence, the general solution of (17) given by (18) becomes

$$\phi(R)=A_1 J_0\left(\beta_{T_f}R\right)-\frac{i\lambda U_0\,\mathrm{Pr}\,J_0(\beta_v R)}{\omega\left(\beta_v^2-\beta_{T_f}^2\right)J_0(\beta_v)}-\frac{i\lambda U_0\,\mathrm{Pr}}{\omega\beta_{T_f}^2}$$

Therefore $T_f(R,x,\tau)$ becomes

$$T_f(R,x,\tau)=\gamma x+\gamma\,\mathrm{Re}\left\{\left[A_1 J_0\left(\beta_{T_f}R\right)-\frac{i\lambda U_0\,\mathrm{Pr}\,J_0(\beta_v R)}{\omega\left(\beta_v^2-\beta_{T_f}^2\right)J_0(\beta_v)}-\frac{i\lambda U_0\,\mathrm{Pr}}{\omega\beta_{T_f}^2}\right]e^{-i\tau}\right\},$$

$$A_1=\frac{i\lambda\,\mathrm{Pr}\,U_0\beta_v\left[B_1\beta_{T_w}+\beta_{T_f}J_1(\beta_v)\right]}{\omega\left(\beta_v^2-\beta_{T_f}^2\right)\beta_{T_f}^2J_0(\beta_v)J_1\left(\beta_{T_f}\right)}$$

$$B_1=\frac{B_2B_3}{B_4+B_5}$$

$$B_2=-\beta_v J_1\left(\beta_{T_f}\right)J_0(\beta_v)+\beta_{T_f}J_0\left(\beta_{T_f}\right)J_1(\beta_v)$$

$$B_3=J_1\left(\beta_{T_w}\right)Y_1\left(\beta_{T_w}(1+2\varepsilon)\right)-J_1\left(\beta_{T_w}(1+2\varepsilon)\right)Y_1\left(\beta_{T_w}\right)$$

$$B_4=k\beta_{T_f}J_1\left(\beta_{T_f}\right)\left[\begin{matrix}J_0\left(\beta_{T_w}\right)Y_1\left(\beta_{T_w}(1+2\varepsilon)\right)\\-J_1\left(\beta_{T_w}(1+2\varepsilon)\right)Y_0\left(\beta_{T_w}\right)\end{matrix}\right]$$

$$B_5=-\beta_{T_w}J_0\left(\beta_{T_f}\right)\left[\begin{matrix}J_1\left(\beta_{T_w}\right)Y_1\left(\beta_{T_w}(1+2\varepsilon)\right)\\-J_1\left(\beta_{T_w}(1+2\varepsilon)\right)Y_1\left(\beta_{T_w}\right)\end{matrix}\right]$$

We also assume that $T_s(R,x,\tau)=\gamma\,\mathrm{Re}\left(x+\chi(R)e^{-i\tau}\right)$

Using this in (12), (12) gives

$$\frac{d^2\chi(R)}{dR^2}+\frac{1}{R}\frac{d\chi(R)}{dR}+i\alpha^2\sigma\,\mathrm{Pr}\,\chi(R)=0 \qquad (19)$$

which is a homogeneous zeroth order Bessel equation.

The general solution of (19) is given by

$$x(R) = A_3 J_0\left(\beta_{T_w} R\right) + A_4 Y_0\left(\beta_{T_w} R\right),$$

$$\beta_{T_w}^2 = i\alpha^2 \sigma \,\mathrm{Pr}$$

Therefore $T_s(R,x,\tau)$ becomes

$$T_s\left(R,x,\tau\right) = \gamma x + \gamma \,\mathrm{Re}\left\{\left[A_3 J_0\left(\beta_{T_w} R\right) + A_4 Y_0\left(\beta_{T_w} R\right)\right] e^{-i\tau}\right\},$$

$$A_3 = \frac{i\lambda \,\mathrm{Pr}\, U_0 \beta_v k Y_1\left(\beta_{T_w}\left(1+2\varepsilon\right)\right) B_1}{\omega \beta_{T_f}\left(\beta_v^2 - \beta_{T_f}^2\right) J_0\left(\beta_v\right) B_3}$$

$$A_4 = \frac{-i\lambda \,\mathrm{Pr}\, U_0 \beta_v k J_1\left(\beta_{T_w}\left(1+2\varepsilon\right)\right) B_1}{\omega \beta_{T_f}\left(\beta_v^2 - \beta_{T_f}^2\right) J_0\left(\beta_v\right) B_3}$$

2.1 Enhanced Thermal Diffusivity

In order to find the enhanced heat transfer that takes place between the hot and cold streams of the tube, we calculate the effective thermal diffusivity. By neglecting the small contribution due to axial thermal conduction (Kurzweg 1985b), the effective averaged thermal diffusivity can be defined as

$$\kappa_e \gamma = -\frac{\omega}{2\pi a^2} \int_0^{\frac{2\pi}{\omega}} dt \int_0^a \mathrm{Re}\left[T\left[r,x,t\right]\right] \mathrm{Re}\left[u(r,t)\right] r\, dr dt \tag{20}$$

where Re represents the real part of the corresponding variable.

It may be noted here that the left and right hand sides of (20) represent the effective axial heat flux per unit cross sectional area and the time averaged convective heat flux produced by the interaction of the cross - stream varying velocity and temperature profiles respectively.

Substituting the expressions for T and u into (20) and performing the time integration leads to

$$\kappa_e = \frac{1}{4} U_0 \int_0^1 \mathrm{Re}\left[\bar{f} V + f \bar{V}\right] dR \tag{21}$$

$$= \frac{U_0^2 \lambda^2 \,\mathrm{Pr}}{4\omega\alpha^2}\left(B_6 + \bar{B}_6 + B_7 + \bar{B}_7\right), \tag{22}$$

$$B_6 = \frac{\beta_{T_w} \beta_v B_1 B_8}{\beta_{T_f}^2\left(\beta_v^2 - \beta_{T_f}^2\right) J_0\left(\beta_v\right) J_1\left(\beta_{T_f}\right)}$$

$$B_7 = \frac{J_1\left(\beta_{T_f}\right)}{\beta_{T_f}} - \frac{\left[-\bar{\beta}_v J_0\left(\beta_{T_f}\right) J_1\left(\bar{\beta}_v\right) + \beta_{T_f} J_1\left(\beta_{T_f}\right) J_0\left(\bar{\beta}_v\right)\right]}{\left(\beta_{T_f}^2 - \bar{\beta}_v^2\right) J_0\left(\bar{\beta}_v\right)}$$

$$B_8 = \frac{1}{\left(\beta_v^2 - \beta_{T_f}^2\right)} \frac{J_1\left(\beta_v\right)}{J_0\left(\beta_v\right)} \left\{ \frac{-\beta_v}{\beta_{T_f}^2 - \bar{\beta}_v^2} - \frac{\beta_v\left(\beta_v^2 - \beta_{T_f}^2\right)}{\left(\bar{\beta}_v^2 - \beta_v^2\right)\left(\bar{\beta}_v^2 - \beta_{T_f}^2\right)} + \frac{\beta_v}{\beta_v^2 - \bar{\beta}_v^2} + \frac{\beta_v \bar{\beta}_v J_0\left(\beta_{T_f}\right) J_1\left(\bar{\beta}_v\right)}{\beta_{T_f}\left(\beta_{T_f}^2 - \bar{\beta}_v^2\right) J_1\left(\beta_{T_f}\right) J_0\left(\bar{\beta}_v\right)} \right\}$$

The non dimensional effective thermal diffusivity is given by

$$\kappa_e^* = \frac{\kappa_e}{\omega\left(\Delta x\right)^2} = \frac{\alpha^2 \,\mathrm{Pr}\left(B_6 + \bar{B}_6 + B_7 + \bar{B}_7\right)}{16\left|\left(1 - \frac{2J_1\left(\beta_v\right)}{\beta_v J_0\left(\beta_v\right)}\right)^2\right|}$$

3. PHYSICAL AND THERMAL PROPERTIES OF THE FLUID AND SOLID

As the physical and thermal properties of the aqueous solution of CPyCl/NaSal are not available in the literature, experiments have been performed, the measurements were made at room temperature (298.15 K).

3.1 Data Obtained by Experiment

Thermal conductivity, thermal diffusivity and the specific heat capacity of the fluid were measured at Indian Institute of Technology at Chennai by the Hot Disk TPS 500 Thermal Conductivity Analyzer using Transient Plane Source (T PS) method. The dynamic viscosities of the fluids were measured with an Anton Paar DSA 5000 M LOVIS 2000 M Micro-viscometer at IIT Chennai. The molar ratios (R_M) of the concentration of NaSal to those of CPyCl are fixed at 0.1, 0.4 and 7. The weight percentage of CPyCl used is 3.6 g (Ali and Swapan Saha 2011) and its concentration is fixed as 100 mmol. The weight percentage of NaSal for three different concentrations namely, 10 mmol, 40 mmol and 700 mmol are 1.601 g, 6.404 g and 112.07 g respectively. The corresponding weight of the aqueous solution of CPyCl/NaSal was measured using a weighing machine for three different volumes (5 ml, 10 ml and 20 ml) of the fluid. The corresponding densities of the fluid samples were calculated by dividing the weights by the volumes of the fluids. Then the average densities were calculated for each sample. The data obtained by the experiments are presented in Table 1. The corresponding Prandtl numbers and the Deborah numbers of the fluids are also presented in Table 1.

Table 1 Physical and thermal properties of the fluids obtained by experiments

Properties		Fluid	
	$R_M = 0.1$	$R_M = 0.4$	$R_M = 7$
$\mu(Pas)$	0.00124	0.00120	0.03768
$\rho(kg/m^3)$	922.98	934.95	1201.6
$k_f(W/mK)$	0.6248	0.4781	0.258
$\kappa_f(10^{-6}m^2/s)$	0.126	0.3263	0.02526
Pr	10.6823	7.43907	1241.25
De	0.26919	0.25621	6.27081

3.2 Data Obtained From the Literature

The fluid relaxation time (t_m) is assumed to be 1.25 s (Lambert, Cuevas, Del Rio, and de Haro 2009). The radius of the tube (a) is varied from 2.5mm to 5mm which corresponds to the micro channel heat exchangers and half the wall thickness (b) is varied from 2 mm to 2.5 mm. Accordingly ε $(= b/a)$ varies from 0.4 to 1. The frequency of oscillation (f) is varied from 10^{-5} *Hertz* to 50 *Hertz*. The corresponding ranges of Womersley number (α) are 0.017 to 38.19 for $R_M = 0.1$; 0.018 to 39 for $R_M = 0.4$ and 0.003 to 7.91 for $R_M = 7$. The thermal conductivities (W/mK) of the above mentioned wall materials (acrylic, glass and AISI 316 stainless steel) are 0.21, 1.38 and 18.3 and the corresponding thermal diffusivities (m^2/s) are 0.12 x 10^{-6}, 0.85 x 10^{-6} and 4.04 x 10^{-6} respectively. All the results obtained in the present analysis are qualitatively same for various concentrations of the aqueous system and wall materials. It is found that the effective thermal diffusivity is higher for all the concentrations of the aqueous system with stainless steel wall. Hence the results are presented for all the concentrations of the aqueous system only with stainless steel wall.

4. RESULTS AND DISCUSSION

The objective of the present investigation is to study the combined effect of conjugation and oscillation on the enhancement of heat transfer in a laminar flow of viscoelastic fluids in circular tubes. In this analysis, we have used the aqueous solution of cetylpyridinium and sodium salicylate (CPyCl/NaSal), a well known surfactant salt system as the heat carrier and acrylic, glass and AISI 316 stainless steel as the wall materials which are compatible with this fluid. This particular solution exhibits an excellent Maxwellian behavior in the temperature range between 20°C and 40°C (Oelschlaeger, Schopferer, Scheffold, and Willen-bacherK 2009).

4.1 Womersley Number

The effect of the Womersley number (α) on the effective thermal diffusivity κ_e^* is analysed and is presented in Figs. 2 - 7. It is observed that there is a critical value (α_c) of α which determines whether the dissipative (viscous) behavior prevails or the resonance appears in the behavior of κ_e^* owing to the elasticity of the fluid. During computation we found that when De = 0, i.e., when the fluid is considered to be viscous, the effect of α on κ_e^* is similar to the results reported earlier by several authors (Kurzweg and De Zhao 1984; Kurzweg 1985a; Kurzweg 1985b; Kurzweg 1986; Kaviany 1986; Inaba, Morita, and Saitoh 2004; Puvaneswari and Shailendhra 2017b) in the case of liquid metals (Newtonian fluids). When De > 0, but when α is small say $\alpha < \alpha_c$, once again we observed that the effect of α on κ_e^* is qualitatively similar to the results reported by the same authors. Therefore, even though De > 0 , the viscoelastic nature of the fluid doesnt change the effect of α on κ_e^* when $\alpha < \alpha_c$. However, when $\alpha > \alpha_c$ (De > 0), we observed the resonant behavior in the effect of α on κ_e^* (Refer Fis 3, 5 and 7 in the present article). Hence, the viscoelastic nature of the fluid alters the effect of α on κ_e^* only when $\alpha > \alpha_c$. The critical values of α for different concentrations of the fluid with different wall materials are presented in Table 2.

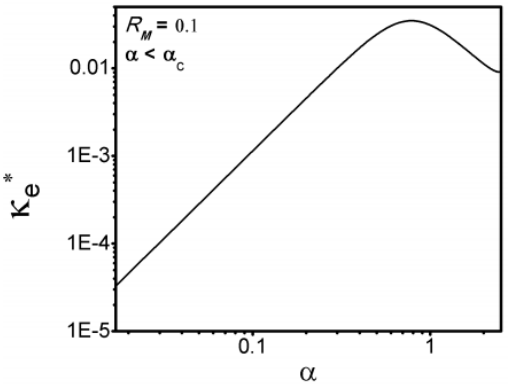

Fig. 2. Effective thermal diffusivity as a function of α for R_M = 0.1 with AISI316 when ε = 1 and α < $α_c$.

Case (i): $\alpha < \alpha_c$

In this case the flow regime is dissipative (viscous) and the fluid behaves like a Newtonian fluid. As α increases κ_e^* first increases, reaches a peak and then decreases (Refer Figs. 2,4,6). This result is similar to the result we have observed in the Newtonian case (Puvaneswari and Shailendhra 2017b). The maximum value of κ_e^* observed in this case is 0.039 when R_M = 0.4 and the wall material is stainless steel.

Table 2. Critical values of the Womersley number

Fluid		Wall Material		
		Acrylic	Glass	AISI316
$R_M = 0.1$	α_C	2.40	2.43	2.48
$R_M = 0.4$	α_C	2.38	2.50	2.56
$R_M = 7$	α_C	1.12	1.12	1.12

Case (ii):$\alpha > \alpha_c$

In this case the system switches from a viscous regime to an elastic regime. The fluid behaves like a non Newtonian fluid and the elastic behavior of the fluid is dominant. A resonant behavior is observed in this case and several maxima occur in κ_e^* at certain values of α (Refer Figs. 3,5,7). It has been observed that the mean flow rate obtained with viscoelastic fluid flows driven by zero mean oscillatory pressure gradient is very much higher than that obtained with ordinary fluids. There is a drastic enhancement in the velocity amplitude at certain frequencies and the maximum velocity is obtained at the smallest resonance frequency (Yu A. Andrienko and Yanovsky 2000). This dramatic enhancement in the mean flow rate contributes to the enhancement of heat transfer. Also, when the frequency increases, the magnitude of the enhancement decreases (Yu A. Andrienko and Yanovsky 2000). Similar result is obtained in the present study. Moreover, the inertial effects dominate the fluid flow characteristics only at high frequencies (Siginer 1991) where resonance appears in the fluid velocity as well as in κ_e^*. Hence, resonance behavior is an inertial phenomenon happening only at large frequencies ($\alpha > \alpha_c$). It is observed that these irregular peaks in the graph of κ_e^* increase up to an optimum value of α (α_p) and decrease beyond that. κ_e^* is maximized at α_p where the fluid flow exhibits a resonant behavior. The maximum value of κ_e^* and the corresponding optimum value of α are presented in Table 3. From Table 3. it is clear that the maximum value of κ_e^* is observed for $R_M = 7$ with the stainless steel wall material and the maximum value is 0.454. Also the maximum value of κ_e^* obtained in this case is 15 times greater than that obtained for $\alpha < \alpha_c$ for the fluid with $R_M = 7$.

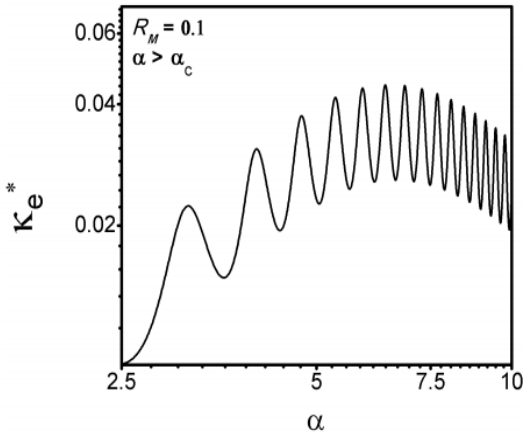

Fig. 3. Effective thermal diffusivity as a function of α for R_M = 0.1 with AISI316 when ε = 1 and α > α_c.

To understand the different effects of α on κ_e^* for $\alpha < \alpha_c$ and $\alpha > \alpha_c$, we analysed the effect of α on the average velocity (AV) of the fluid as the velocity typically has the greatest affect on κ_e^*. The results obtained are physically interpreted as follows.

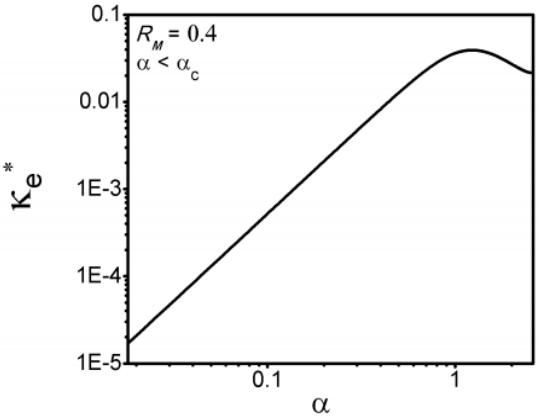

Fig. 4. Effective thermal diffusivity as a function of α for R_M = 0.4 with AISI316 when ε = 1 and α < α_c.

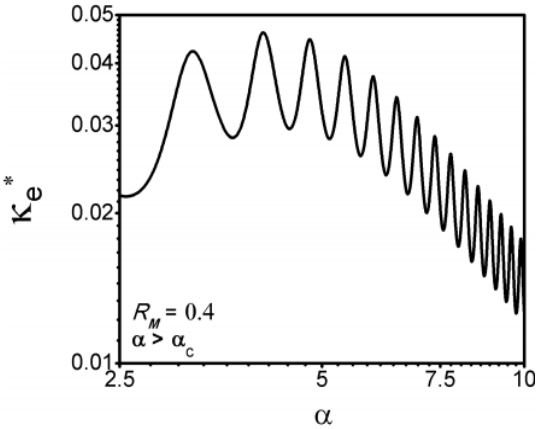

Fig. 5. Effective thermal diffusivity as a function of α for R_M = 0.4 with AISI316 when ε = 1 and α > α_c.

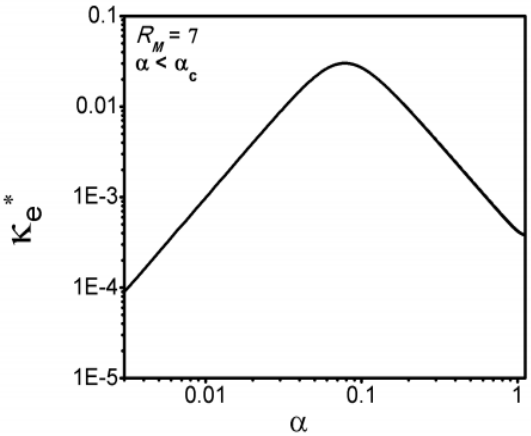

Fig. 6. Effective thermal diffusivity as a function of α for R_M = 7 with AISI316 when ε = 1 and α < α_c.

Table 3 Effective thermal diffusivity (κ_e^*) and optimum values of the Womersley number

Fluid		Wall Material		
		Acrylic	Glass	AISI316
$R_M = 0.1$	κ_e^*	0.042	0.043	0.045
	αp	6.84	6.38	6.38
$R_M = 0.4$	κ_e^*	0.041	0.043	0.046
	αp	4.07	4.08	4.09
$R_M = 7$	κ_e^*	0.452	0.453	0.454
	αp	7.90	7.90	7.90

Womersley number is used to describe whether the resulting fluid flow is quasi-steady or not. It measures the ratio of transient inertial force to the viscous force. When $\alpha < \alpha_c$ the viscous force dominates over the elastic force and the velocity profiles exhibit a parabolic shape such that the fluid oscillating with the greatest amplitude is farthest from the walls (quasi-steady behavior). Therefore the average velocity (AV) and hence κ_e^* behaves like those for a Newtonian fluid. On the other hand, when $\alpha > \alpha_c$, the velocity profiles are no longer parabolic and the flow is phase-shifted in time relative to the oscillating pressure gradient. In this case, the fluid moves like a solid block which means that the elastic effects of the fluid dominate the flow. As a result, resonance appears in AV and hence in κ_e^* when $\alpha > \alpha_c$. For further details on this result, one may refer to Loudon *et al* (Loudon and Tordesillas 1998).

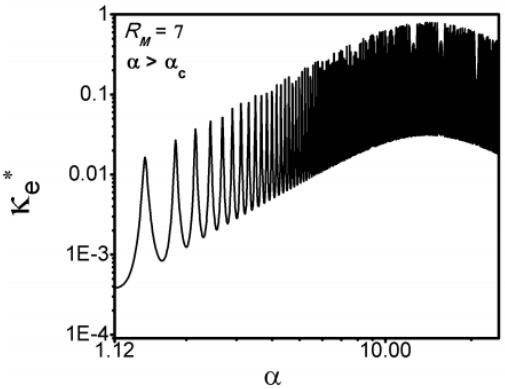

Fig. 7. Effective thermal diffusivity as a function of α for R_M = 7 with AISI316 when ε = 1 and α > $α_c$.

4.2 Wall Thermal Conductivity

Figs. 8-10 show the effect of wall thermal conductivity on κ_e^* for R_M = 0.1, R_M = 0.4 and R_M = 7 respectively. When $\alpha < \alpha_c$, as k_s increases κ_e^* also increases only after a certain value of α whatever may be the wall thickness. This result is in good agreement with the results reported by Kurzweg (Kurzweg and De Zhao 1984) and Inaba *et al* (Inaba, Morita, and Saitoh 2004) in the Newtonian case.

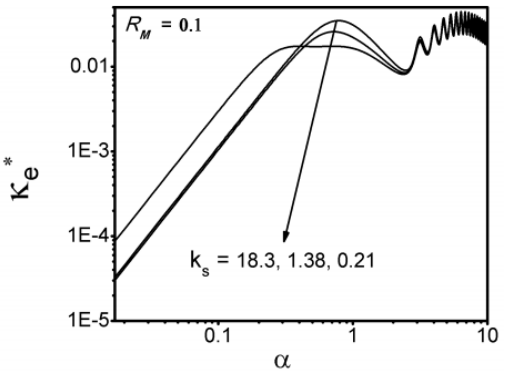

Fig. 8. Effect of k_s on κ_e^* for R_M = 0.1 with AISI316 when ε = 1.

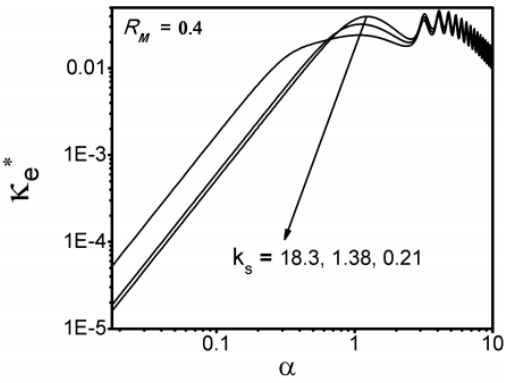

Fig. 9. Effect of k_s on κ_e^* for R_M = 0.4 with AISI316 when ε = 1.

In our recent work (Puvaneswari and Shailendhra 2017b) with liquid metals, we have found that when the frequency is large κ_e^* increases with increasing k_s whatever may be the wall thickness whereas in the case of optimum frequency the same result is obtained only beyond a certain wall thickness. However the above observations are not valid in the case of low frequency. Hence the results obtained in the present study are consistent with our earlier results except for the optimum frequency case with small ε.

On the other hand, when $\alpha > \alpha_c$, k_s has an insignificant effect on κ_e^* at any wall thickness (Refer Figs 8-10). Hence, the conjugation effect is dominated by the elastic effects of the fluid except where the peak values are observed in the resonant behavior of κ_e^*. In this case, the resonance behavior of κ_e^*, observed with a large number of peaks, is same for all the wall materials. Even though all the curves for different k_s merge in this case, the peaks are slightly different for different k_s and th

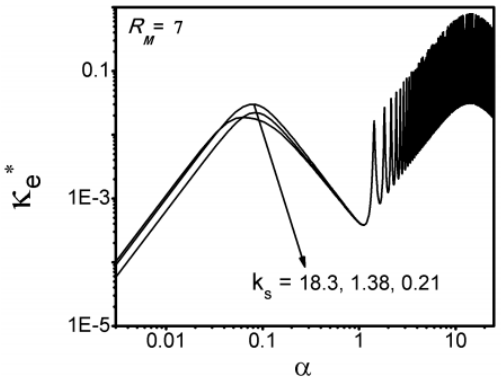

Fig. 10. Effect of k_s on κ_e^* for R_M = 7 with AISI316 when ε = 1.

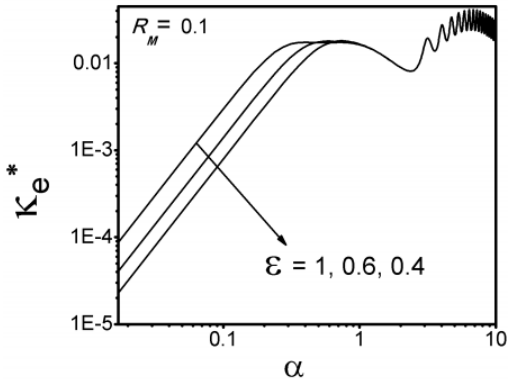

Fig. 11. Influence of wall thickness on κ_e^* for R_M= 0.1 with AISI316.

maximum peak is observed for all the fluids with the stainless steel wall.

In the insulated case of wall materials, Lambert *et al* (Lambert, Cuevas, and Del Rio 2006) observed that in the Newtonian case, the maxima occur at different α for different fluids whereas in the viscoelastic case, the maxima occur at the same α for each fluid with Deborah numbers ≥ 1. However we observed that the maxima occur at different α for each fluid in both viscous and elastic regimes. Moreover Lambert *et al* (Lambert, Cuevas, and Del Rio 2006) mentioned that the magnitude of maximum κ_e^* is approximately same for Newtonian fluids but different for viscoelastic fluids. We observed that the maximum value of κ_e^* is different for all the fluids in both viscous and elastic regimes. Therefore we are in agreement with Lambert *et al* (Lambert, Cuevas, and Del Rio 2006) only in the case of viscous regime.

4.3 Wall Thickness

In the Newtonian case, Kurzweg (Kurzweg 1985b) showed that κ_e^* is independent of wall thickness in the high frequency limit. Kaviany (Kaviany 1986) observed that κ_e increases with increasing ε when the frequency is small. Inaba *et al* (In-aba, Morita, and Saitoh 2004), Puvaneswari and Shailendhra (Puvaneswari and Shailendhra 2016) and Puvaneswari and Shailendhra (Puvaneswari and Shailendhra 2017a) proved that the heat flux is increased when ε is increased but the effect is saturated beyond a certain wall thickness whatever may be the frequency.

In the present study, in the case of viscoelastic fluid, it is observed that in the viscous regime ($\alpha < \alpha_c$), κ_e^* increases as ε is increased whereas as in the elastic regime ($\alpha > \alpha_c$), the effect of ε on κ_e^* is saturated (Refer Figs. 11-13). When $\alpha > \alpha_c$, the conjugation effect is suppressed by the elastic effects of the fluid and hence κ_e^* is independent of wall thick-ness (Refer Figs. 11-13). The result we obtained in the viscous regime is consistent with the

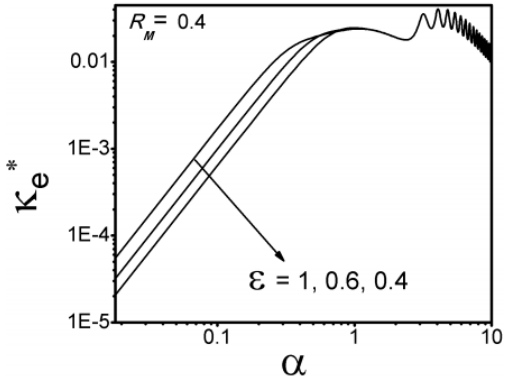

Fig. 12. Influence of wall thickness on κ_e^* for R_M= 0.4 with AISI316.

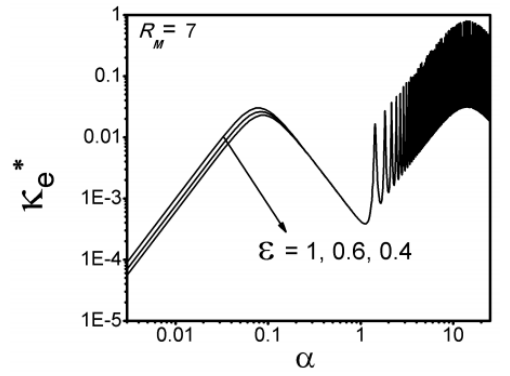

Fig. 13. Influence of wall thickness on κ_e^* for R_M= 7 with AISI316.

literature. Moreover in the viscous regime a maximum increase of 50.63% in κ_e is obtained by increasing the wall thickness for the fluid with R_M = 7 with stainless steel wall which is higher than that (46.14%) obtained by Puvaneswari and Shailendhra (Puvaneswari and Shailendhra 2016) in the Newtonian case.obtained in the viscous regime is consistent with the literature. Moreover in the viscous regime a maximum increase of 50.63% in κ_e is obtained by increasing the wall thickness for the fluid with R_M = 7 with stainless steel wall which is higher than that (46.14%) obtained by Puvaneswari and Shailendhra (Puvaneswari and Shailendhra 2016) in the Newtonian case.

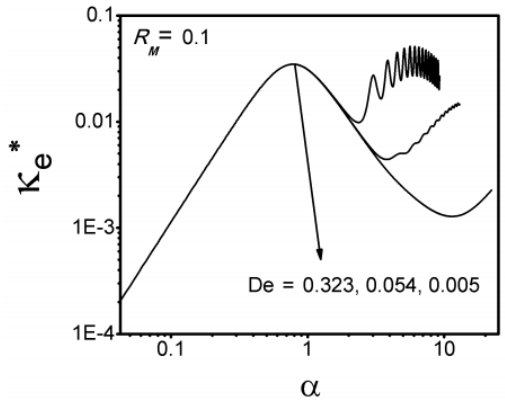

Fig. 14. κ_e^* as a function of α for different Deborah numbers for R_M = 0.1 with AISI316.

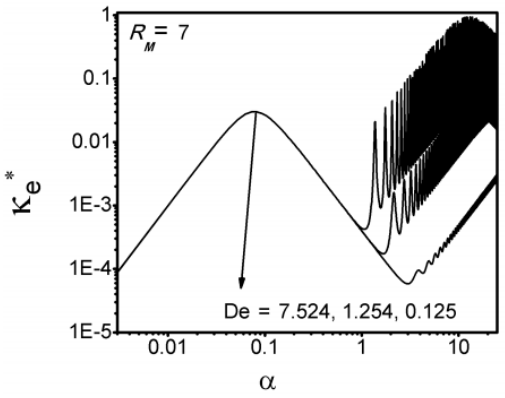

Fig. 16. κ_e^* as a function of α for different Deborah numbers for R_M = 7 with AISI316.

4.4 Deborah Number

The Deborah number (De) incorporates both the elasticity and viscosity of the fluid. When De is small elastic effects can be neglected and the fluid is treated as a purely viscous fluid whereas in the case of high De, elastic effects dominate. The influence of the fluid relaxation time and thus the effect of the Deborah number on κ_e^* is illustrated in Figs. 14-16 for all the fluids with stainless steel wall material when t_m = 0.025, 0.25 and 1.5 sec. The corresponding values of De are shown in figures. From the figures it is clear that when $\alpha < \alpha_c$ there is no change in κ_e^* with respect to the Deborah number. In this case, as the fluid behaves like a Newtonian fluid, κ_e^* is independent of the fluid relaxation time. However when $\alpha > \alpha_c$, the maximum value of κ_e^* increases with increasing De. In other words, as the fluid relaxation time (t_m) increases, maximum κ_e^* also increases. These results are in good agreement with Lambert *et al* in the insulated case (Lambert, Cuevas, and Del Rio 2006).

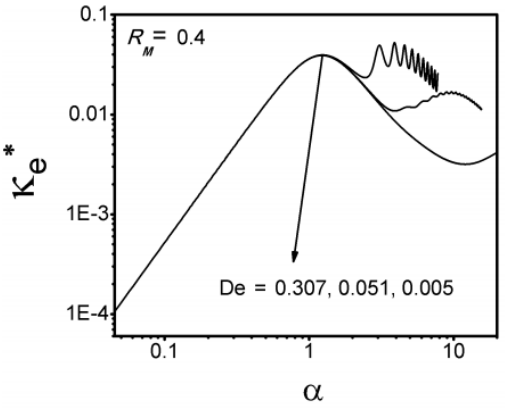

Fig. 15. κ_e^* as a function of α for different Deborah numbers for R_M = 0.4 with AISI316.

4.5 Fluid Width

The fluid width can't be made very large as the thermal energy storage-release process is based on heat diffusion across the pipe. With water as the woring fluid and aluminum as the wall material Kaviany (Kaviany 1986) investigated the effect of the half channel width, a, on the effective thermal diffusivity when ω = 10 rad/s, A_0 = 6.6 x 104 N/m^3 and ε = 2. He reported that κ_e^* increases with in-creasing *a*, attains a peak and then decreases. We have done the same analysis for all the fluid and wall combinations at different frequencies. How-ever, the results are presented in Fig. 17 only for R_M = 0.1 with steel wall to minimize the number of pages.

From Fig. 17, it is clear that the behavior of κ_e^* is similar to that of a Newtonian fluid in the case of low frequency. When the frequency is medium, there is a critical value of *a* up to which κ_e^* behaves in the same manner as the Newtonian fluid and after which it exhibits resonance behavior due to the elasticity of the fluid. Also, when the frequency is large, elastic effects of the fluid alone decide the heat transfer characteristics. Therefore, the effect of *a* on κ_e^* depends on the frequency of oscillation.

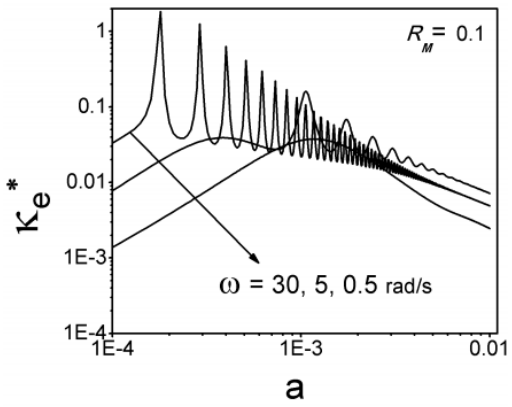

Fig. 17. Effect of half the fluid width on κ_e^* for R_M = 0.1 with AISI316.

Also not only frequency (or α) but also *a* is the deciding factor for the occurrence of resonance in the graph of κ_e^* and hence for the elastic effects to dominate over the viscous effects. It is clear from Fig. 17 that it is better to keep the value of a corresponding to the first peak in the elastic regime as the optimum value of *a* to maximize the heat transfer rate.

5. TOTAL HEAT FLUX TRANSPORTED BY THE FLUID

To get a quantitative estimation of the enhancement of heat transfer, we compared the axial heat flux due to oscillation (Q(W/m^2)) with the purely molecular heat flux (Qm(W/m^2)) in the same direction. For a given temperature gradient γ,

$$Q = -\rho_f c_f \kappa_e \gamma \quad = -\rho_f c_f \kappa_f \widehat{\kappa_e} \gamma \quad = -k_f \widehat{\kappa_e} \gamma$$

$$Q_m = -k_f \gamma$$

Here, $\widehat{\kappa_e} = \frac{\kappa_e}{k_f}$ is the non dimensional effective thermal diffusivity of the fluid. Therefore, the ratio of the heat fluxes Q and Q_m becomes

$$\frac{Q}{Q_m} = \frac{-k_f \widehat{\kappa_e} \gamma}{-k_f \gamma} = \widehat{\kappa_e}$$

Hence the heat flux transported by oscillation becomes $Q = -\widehat{\kappa_e} k_f \gamma$ *(W/m²)* .

Table 4. Heat flux transported by viscoelastic fluid

R_M		Wall Material		
		Acrylic	Glass	AISI316
0.1	Thermally Insulated (W/m^2)	1.59 1.24 ×10^8	1.59 1.24 ×10^8	1.59 1.24 ×10^8
	Thermally Conducting (W/m^2)	1.60 6.50 ×10^7	1.39 5.79 ×10^7	1.40 6.07 ×10^7
0.4	Thermally Insulated (W/m^2)	0.53 1.09 ×10^7	0.53 1.09 ×10^7	0.53 1.09 ×10^7
	Thermally Conducting (W/m^2)	0.54 6.31 ×10^6	0.54 6.72 ×10^6	0.55 7.23 ×10^6
7	Thermally Insulated (W/m^2)	220 6.53 ×10^{11}	220 6.53 ×10^{11}	220 6.53 ×10^{11}
	Thermally Conducting (W/m^2)	49.8 0.45 ×10^{10}	49.8 4.52 ×10^{10}	49.8 4.54 ×10^{10}

The heat flux Q corresponding to the maximum value of effective thermal diffusivity and the corresponding optimum values of α and ε is calculated using Δx = 1 *m* (Kurzweg 1985b) and a = 2.5 *mm* for both Newtonian and viscoelastic fluids and is presented in Tables 4-5 in which the first entry in each box represents the frequency *f* (*Hertz*) and the second entry represents the heat flux *Q* (*W/m²*). Here, the frequency of oscillation f is obtained from *ω* corresponding to the optimum value of α when *a* = 2.5 *mm*. As the fluid under consideration is an aqueous solution, we have used the temperature gradient of water as the temperature gradient of the fluid namely, γ = 31.25 *K/m* when the length of the tube is 3.2 *m*. From Tables 4-5 it is clear that, in the case of Newtonian fluid (liquid metal) *Na* a high heat flux of 2.19 x 108 *W/m²* is achieved with the thermally conducting wall material Ni whereas in the case of viscoelastic fluid (R_M = 7), the maximum heat flux of 6.53 x 1011 *W/m²* is obtained with the insulated wall. In viscoelastic fluids, though the heat flux obtained in the insulated case is higher, the corresponding frequency of oscillation (*f* = 220 Hertz) is very large. How-ever, a maximum heat flux of 4.54 x 1010 *W/m²* can be achieved with thermally conducting wall material with comparatively less frequency (*f* = 49.83 *Hertz*). Also the maximum heat flux (4.54 x 1010 *W/m²*) obtained by the viscoelastic fluid with the conducting wall is 207 times higher than that (2.19 x 108 *W/m²*) obtained by the Newtonian fluid (liquid metal). Hence, the present study demonstrates that viscoelastic fluids are the suitable working flu-ids in the conjugate heat transfer problems pertaining to the enhancement of heat transfer.

Table 5 Heat flux transported by Newtonian fluid

Fluid		Wall Material		
		Ni	*Nb*	*AISI316*
K	Thermally Insulated *(W/m²)*	3.42 4.63 ×10^5	3.42 4.63 ×10^5	3.42 4.63 ×10^5
	Thermally Conducting *(W/m²)*	8.46 1.38 ×10^8	7.65 1.21 ×10^8	7.05 1.05 ×10^8
Na	Thermally Insulated *(W/m²)*	3.41 1.35 ×10^6	3.41 1.35 ×10^6	3.41 1.35 ×10^6
	Thermally Conducting *(W/m²)*	6.45 **2.19** ×10^8	5.31 1.74 ×10^8	4.49 1.34 ×10^8
NaK	Thermally Insulated *(W/m²)*	2.64 9.05 ×10^5	2.64 9.05 ×10^5	2.64 9.05 ×10^5
	Thermally Conducting (W/m^2)	5.48 1.29 ×10^8	4.97 1.14 ×10^8	4.57 0.99 ×10^8

It should be noted here that, Kurzweg (Kurzweg 1985b) obtained a high heat flux of 1.8 x 1010 *W/m²* using pressurized water when *ω* = 300 *rad/s*. In our earlier work (Puvaneswari and Shailendhra 2017b) with liquid metals, we were able to achieve

such a high heat flux for ω = 300 rad/s only when Δx = 3.1 m. Here also if we choose such a large value for Δx instead of Δx = 1 *m*, we can achieve a high heat flux of 1.56 x 10^{10} W/m^2 for the fluid *Na* with the wall material *Ni* which is two orders of magnitude higher than that obtained with Δx = 1 *m*.

6. COMPARISON WITH EARLIER RESULTS

All the results reported in Kurzweg (Kurzweg 1985b) for three different values of *Pr* namely, *Pr* = 1000, *Pr* = 100 and *Pr* = 0.1 can be recovered from the present investigation by taking the limit as *De* → 0 while using the same values for all the parameters as those of Kurzweg. The results for the viscoelastic fluid with an insulated wall reported by Lambert *et al* (Lambert, Cuevas, and Del Rio 2006) can be retrieved from the present work when $k = k_f/k_s \rightarrow \infty$.

In the insulated case, with a 40:40 concentration of the same fluid, Lambert *et al* (Lambert, Cuevas, and Del Rio 2006) obtained a maximum $\widehat{\kappa_e}$ of 12 when a = 0.025 *m*, μ = 30 *Pas*, ρ = 1005 kg/m^3, t_m = 1.25 *s*, *Pr* = 1000 and De = 59.7. As the thermal conductivity of the fluid was not available during their investigation, they considered Prandtl numbers to be one and two orders of magnitude higher than that of water namely, *Pr* = 100 and *Pr* = 1000 in their study and showed that due to oscillation the effective thermal diffusivity is increased by 12 times than that existing in the absence of oscillations. But we have done experiments, got the exact values for all the physical and thermal properties of the fluid and used them in the present study. With the conducting wall materials, we have shown that because of oscillation, the effective thermal diffusivity (κ_e) is increased by 5.63 ×109 times than that existing in the absence of oscillations (Refer Table 6.) and the maximum enhancement is observed for R_M = 7 with the stainless steel wall material. This increase in κ_e is much higher than that (1.84 x 104 times) obtained for the Newtonian fluid *NaK* with nickel wall (Refer Table 7.). Hence, viscoelastic fluids are the suitable working fluids for the augmentation of heat transfer in dream pipe with a thermally conducting wall.

Table 6 $\widehat{\kappa_e}$ for viscoelastic fluid with thermally con-ducting wall

R		Wall Material		
		Acrylic	*Glass*	*AISI316*
0.1	$\widehat{\kappa_e}$	3.33 ×10^6	2.97 ×10^6	3.11 ×10^6
0.4	$\widehat{\kappa_e}$	4.22 ×10^5	4.50 ×10^5	4.84 ×10^5
7	$\widehat{\kappa_e}$	5.60 ×10^8	5.61 ×10^9	5.63 ×10^9

Table 7 $\widehat{\kappa_e}$ for Newtonian fluid with thermally conducting wall

Fluid		Wall Material		
		Nickel	Niobium	AISI316
K	$\widehat{\kappa_e}$	1.79 ×10^4	1.57 ×10^4	1.36 ×10^4
Na	$\widehat{\kappa_e}$	1.41 ×10^4	1.11 ×10^4	8.61 ×10^3
NaK	$\widehat{\kappa_e}$	1.81 ×10^4	1.62 ×10^4	1.40 ×10^4

7. CONCLUSION

The combined effects of conjugation and oscillation on the enhancement of heat transfer in a laminar oscillatory flow of viscoelastic fluids in circular tubes with thermally conducting walls are investigated. The thermal properties used in the present analysis were calculated by conducting the required experiments. The main results obtained are summarized as follows.

- There is a critical value of α up to which the fluid behaves like a Newtonian fluid and after that α the elastic effects of the fluid are dominant and the heat transfer characteristics exhibit a resonant behavior. A maximum κ_e^* of 0.454 is observed when R_M = 7 and the wall is stainless steel. Several maxima occurs in κ_e^* for several resonant frequencies whereas a single maximum occurs for a Newtonian fluid.
- In the viscous regime, κ_e^* increases with in-creasing k_s only after a certain value of α whatever may be the value of wall thickness. However in the elastic regime, the effect of k_s on κ_e^* is insignificant whatever ε may be. Hence the effect conjugation is dominated by the elastic property of the viscoelastic fluid.
- In the viscous regime, κ_e^* increases as ε is increased whereas in the elastic regime, the effect of ε on κ_e^* is saturated as the elastic effects of the fluid dominate over the conjugation effects. Moreover, in the viscous regime a maximum increase of 50.63% in κ_e^* is obtained by increasing the wall thickness for the fluid with R_M = 7 with stainless steel wall which is higher than that (46.14%) obtained in the Newtonian case (Puvaneswari and Shailendhra 2016).
- In the elastic regime, κ_e^* increases with in-creasing De. However in the viscous regime the influence of De on κ_e^* is insignificant as the fluid behaves like a Newtonian fluid (De = 0).
- Larger the molar ratio R_M of concentrations of

counterion to surfactant higher the enhancement of heat transfer.

- In the case of a viscoelastic fluid with a thermally conducting wall, due to oscillation, the effective thermal diffusivity is increased by 5.63x 10^9 times than that existing in the absence of oscillations and this increase is much higher than that (1.84 x 10^4 times) obtained for the Newtonian fluid (liquid metal). Further, the maximum heat flux (4.54 x 10^{10} W/m^2) transported by the viscoelastic fluid with thermally conducting wall is 207 times higher than that (2.19 x 10^8 W/m^2) obtained with the Newtonian fluid. Hence, viscoelastic fluids seem to be preferable working fluids in dream pipes in the conjugate case.
- The combined effect of frequency (or α) and the fluid width (a) is the main reason for the occurrence of resonance in the graph of κ_e^* and hence for the elastic effects to dominate over the viscous effects.
- It is strongly believed that the results reported in the present investigation are useful while designing viscoelastic Dream Pipes and micro channel heat exchangers.

ACKNOWLEDGMENTS

We would like to thank Dr. Ramesh Gardas, Professor of Chemistry in IIT Chennai and his students, Mr. Somenath Panda and Mr. Rabi Narayan Patra for their support and help in conducting the experiments. We also thank Dr. Murali Rangarajan, Associate Professor of Chemical Engineering, Amrita University for his valuable suggestions and Mr. M. Praveen, B. Tech student, Amrita University for helping us to complete the experimental work succesfully.

REFERENCES

Ali, M. and K. Swapan Saha (2011). Hydro- gen bonded large molecular aggregates of charged amphiphiles and unusual rheology: Photochemistry and photophysics of hydroxyaromatic dopants. In *Hydrogen-Bonding and Transfer in the Excited State*, Volume 9, pp. 1–35. John Wiley and Sons.

Chatwin, P. (1975). On the longitudinal dispersion of passive contaminant in oscillatory flows in tubes. *Journal of Fluid Mechanics 71*(03), 513–527.

Inaba, T., G. Morita and K i. Saitoh (2004). Longitudinal heat transfer enhanced by fluid oscillation in a circular pipe with conductive wall. *Heat Transfer Asian Research 33*(2), 129–139.

Kaviany, M. (1986). Some aspects of enhanced heat diffusion in fluids by oscillation. *International Journal of Heat and Mass Transfer 29*(12), 2002–2006.

Kurtcebe, C. and M. Erim (2005). Heat transfer of a viscoelastic fluid in a porous channel. *International Journal of Heat and Mass Transfer 48*(23), 5072–5077.

Kurzweg, U. (1985a). Enhanced heat conduction in fluids subjected to sinusoidal oscillations. *J. Heat Transfer 107*(2), 459–462.

Kurzweg, U. (1985b). Enhanced heat conduction in oscillating viscous flows within parallel-plate channels. *Journal of Fluid Mechanics 156*, 291–300.

Kurzweg, U. (1986). Temporal and spatial distribution of heat flux in oscillating flow subjected to an axial temperature gradient. *International Journal of Heat and Mass Transfer 29*(12), 1969–1977.

Kurzweg, U. and L. De Zhao (1984). Heat transfer by high-frequency oscillations: A new hydrodynamic technique for achieving large effective thermal conductivities. *Physics of Fluids* (1958-1988) 27(11), 2624–2627.

Lambert, A., S. Cuevas and J. Del Rio (2006). Enhanced heat transfer using oscillatory flows in solar collectors. *Solar Energy 80*(10), 1296–1302.

Lambert, A., S. Cuevas, J. Del Rio and M. L. de Haro (2009). Heat transfer enhancement in oscillatory flows of Newtonian and viscoelastic fluids. *International Journal of Heat and Mass Transfer 52*(23), 5472–5478.

Loudon, C. and A. Tordesillas (1998). The use of dimensionless womersley number to characterize the unsteady nature of internal flow. *Journal of theoritical Biology 191*, 63–78.

Naccache, M. F. and P. R. S. Mendes (1996). Heat transfer to non-newtonian fluids in laminar flow through rectangular ducts. *International Journal of Heat and Fluid Flow 17*(6), 613–620.

Oelschlaeger, C., M. Schopferer, F. Scheffold and N. Willenbacher K (2009). Linear-to-branched micelles transition: A rheometry and diffusin wave spectroscopy (dws) study. *Langmuir 25*, 716–723.

Peres, N., A. Afonso, M. Alves and F. Pinho (2009). *Heat transfer enhancement in laminar flow of viscoelastic fluids through a rectangular duct*. In Congreso de M´etodos Num´ericos en Ingenier´ıa.

Pinho, F. and P. Coelho (2006). Fully-developed heat transfer in annuli for viscoelastic flu-ids with viscous dissipation. *Journal of Non-newtonian Fluid Mechanics 138*(1), 7–21.

Puvaneswari, P. and K. Shailendhra (2016). E hancement of heat transfer in a liquid metal flow past a thermally conducting and oscillating infinite flat plate. *Journal of Applied Fluid Mechanics 9*(3), 1395–1407.

Puvaneswari, P. and K. Shailendhra (2017a). Enhancement of heat transfer in a laminar hydromagnetic flow of a liquid metal past a thermally conducting and oscillating in-finite flat plate. *Heat Transfer Asian Research 46*(6), 598–622.

Puvaneswari, P. and K. Shailendhra (2017b). Study of conjugate heat transfer in electro-magnetic liquid metal dream pipe. *Archive of Mechanical Engineering 64*(3), 375–399.

Shailendhra, K. and S. AnjaliDevi (2011). On the enhanced heat transfer in the oscillatory flow of liquid metals. *Journal of Applied Fluid Mechanics 4*(2), 57–62.

Siginer, A. (1991). On some nearly viscometric flows of viscoelastic fluids. *Rheoogical Acta 30*, 447–473.

Siriwatwechakul, W., T. LaFleur, R. K. P. and P. Sullivan (2004). Effects of organic solvents on the scission energy of rod-like micelles. *Langmuir 20*, 8970–8974.

Tatsumi, K., O. Nakajima, W. Nagasaka and K. Nakabe (2012). Flow observation and heat transfer performance of viscoelastic fluid flow in a serpentine channel. ICHMT DIGITAL LIBRARY ONLINE.

Watson, E. (1983). Diffusion in oscillatory pipe flow. *Journal of Fluid Mechanics 133*, 233–244.

Yu A. Andrienko, Siginer, D. and Y. G. Yanovsky (2000). Resonance behavior of viscoelastic fluids in poiseuille flow and application to flow enhancement. *International Journal of Non-Linear Mechanics 35*, 95–102.

Zhou, G. F. and T. Peng (2012). *Heat transfer enhancement of viscoelastic fluid in the rectangle microchannel with constant heat fluxes*. In Applied Mechanics and Materials, Volume 117, 574–581. Trans Tech Publ.